

## CARBONATES' DUAL-PHYSICS MODELING AIMED AT SEISMIC RESERVOIR CHARACTERIZATION

ALIREZA SHAHIN, MICHAEL MYERS and LORI HATHON

*Department of Petroleum Engineering, University of Houston - Downtown, Houston, TX 77002, U.S.A. arshah@gmail.com*

(Received August 29, 2016; revised version accepted May 7, 2017)

### ABSTRACT

Shahin, A., Myers, M. and Hathon, L., 2017. Carbonates' dual-physics modeling aimed at seismic reservoir characterization. *Journal of Seismic Exploration*, 26: 351-365.

Staged Differential Effective Medium (SDEM) models are general techniques for modeling the impact of mineralogy and texture on permeability, resistivity, and acoustic measurements. Independent investigations of resistivity and acoustic properties have been previously addressed the problem for carbonate reservoirs. The literature lacks a jointly optimized model which is proposed in this paper. To further constrain the model parameters in the nonlinear optimization, independent measurements of petrophysical (NMR) and petrographical properties ( $\mu$ CT) are used as inputs to the model.

The calibrated petro-elastic and petro-electric models that we generate allow pore structure to be derived from velocity and resistivity interpretations of well logs. Rock physics templates that are created using SDEM are extremely important to calibrate and interpret pre-stack seismic inversion results.

KEY WORDS: velocity, resistivity, carbonate, staged, differential, effective, model.

### INTRODUCTION

A major portion of world's oil and gas reserves is in carbonate reservoirs. However, the development of forward models for predicting the physical properties of carbonate rocks has not been as successful as similar efforts for clastic reservoirs. This lack of an existing interpretation models for carbonates is thought to be due to several factors.

Modeling the pore geometry and texture of carbonate rocks is usually thought to be more complex than in sandstones. This is a result of the higher chemical reactivity of carbonate minerals and the influence of diagenesis which often plays the primary role in defining the character of a carbonate rock. Previous work has been done for sets of very diverse samples (Myers, 1991; Myers and Hathon, 2012), we expressly calibrate a model for specific field.

Previous experimental studies have concentrated either on elastic or on electrical properties but not both (Myers, 1991; Myers and Hathon, 2012). Integration of these measurements, which are controlled by the same pore structure (vugs versus matrix porosity) are carried out in this paper.

To demonstrate the joint SDEM methodology, we made three independent porosity measurements on carbonate core plugs from northern Niagaran reef. These included Archimedes,  $\mu$ CT, and NMR porosities. We have modeled two pore types: microporosity and vuggy porosity. Vuggy porosity is defined as a pore that is three times the median grain size.

Resistivity, P- and S-wave ultrasonic measurements were made of the same brine saturated core plugs. The joint modeling of resistivity and velocities was performed using SDEM technique originally developed by Myers and Hathon (2012). Initial values and parameter space constraints derived from earlier publications. The modeled vuggy versus matrix porosity is compared to the independently estimated porosities from NMR and  $\mu$ CT. The parameters in the resistivity and velocity models are optimized in a global stochastic optimization algorithm.

## POROSITY MEASUREMENTS

Three independent porosity measurements on carbonate core plugs have been made. These include Archimedes,  $\mu$ CT, and NMR porosities.

In Archimedes technique the weight of core plugs in dry, saturated and submerged conditions, pore volumes and porosity are determined. This technique is still the most accurate method to estimate total porosity. The porosity of core plugs using this method vary between 5 and 16 porosity units.

In  $\mu$ CT technique, X-Rays are utilized to provide high-resolution images of geometry and microstructures. In Fig. 1 vertical and horizontal slices of the 3D volume are displayed. A significant portion of the pore type are vugs and no other visible pore type can be seen using  $\mu$ CT. We performed a segmentation technique using color classification to measure the vuggy porosity of the core plugs. On average,  $\mu$ CT-derived porosities are smaller than those estimated from Archimedes and NMR. This is consistent with the fact that  $\mu$ CT cannot resolve the microporosity.

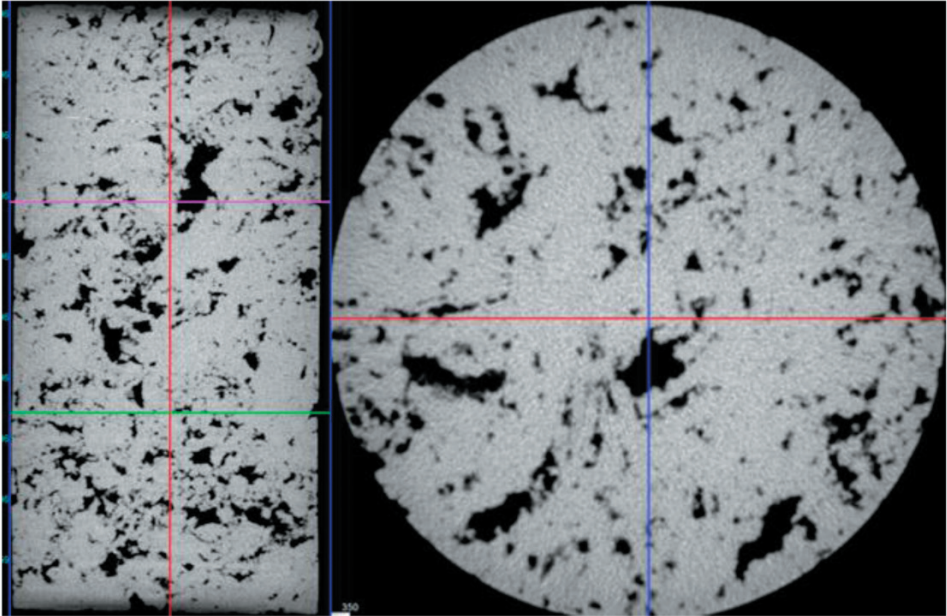


Fig. 1. Micro-CT scan of the carbonate core plug. The left image is a horizontal and the right one is a vertical slice through the 3D image acquired. Note that the majority of the pore volume are vugs and microporosity is not visible.

NMR measures the induced magnet moment of hydrogen nuclei (protons) contained within the fluid-filled pore space of porous media. The NMR measurements for porosity closely follow Archimedes porosities within 1 to 2 porosity unit. The smaller value for the NMR may be due to extremely small pores beyond the resolution of the NMR. Fig. 2 shows the distributions of samples used in this research. To better predict the contribution of each pore type, we chose to fit a Weibull distribution to NMR response. To estimate the model parameters for curve-fitting exercise a non-linear global optimization technique called very fast simulated annealing (VFSA) has been utilized. The detail of VFSA is summarized in the Appendix.

#### NMR $T_2$ -CURVE FITTING EXERCISE USING WEIBULL DISTRIBUTION AND VFSA OPTIMIZATION

We chose to utilize the Weibull distribution as a base function for curve fitting. This is due to the fact that Weibull is a versatile distribution that can take on the characteristics of other types of distributions by varying the value

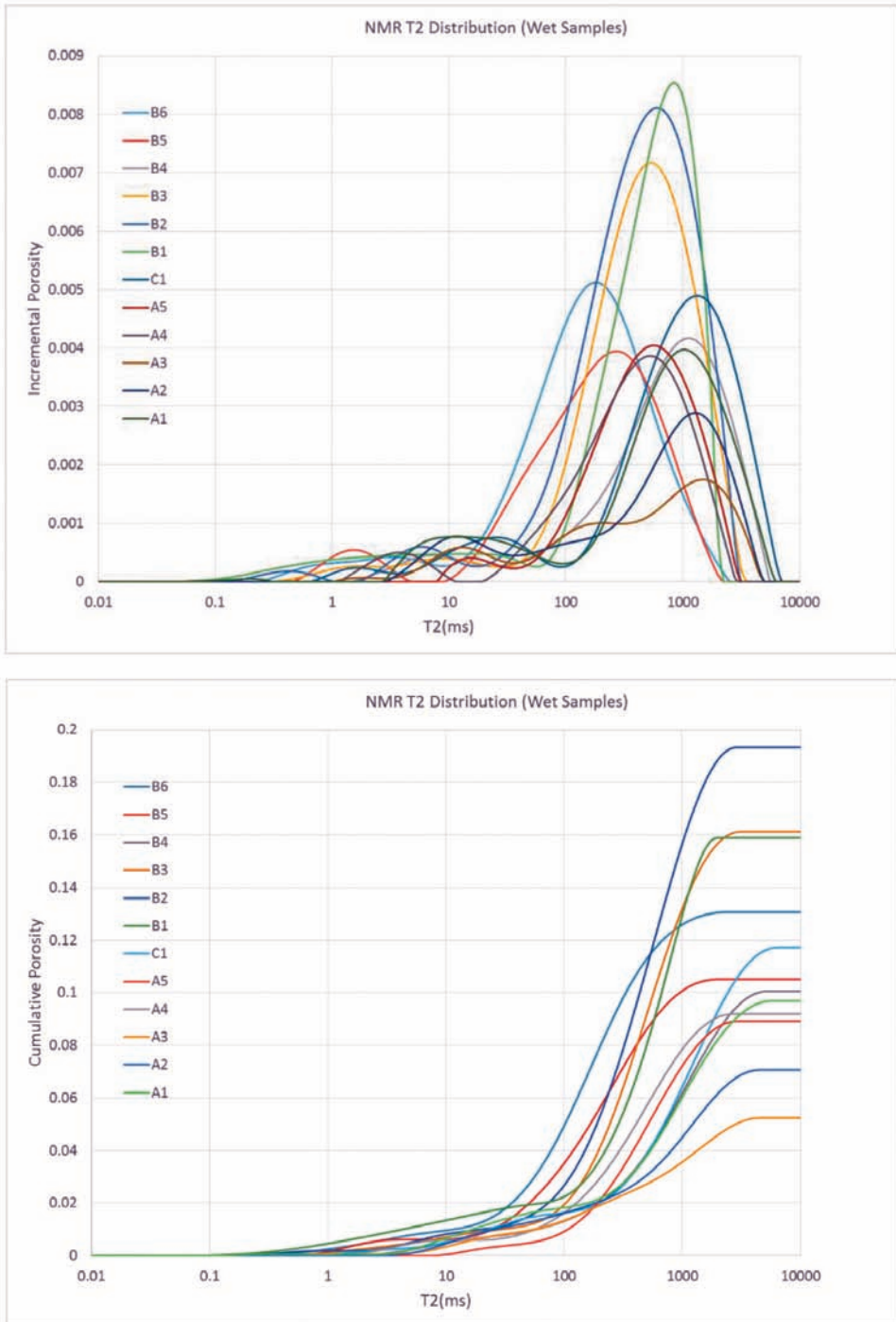


Fig. 2. Top panel shows NMR T<sub>2</sub> distributions of all the samples used in this study. The bottom panel shows the cumulative distribution of NMR T<sub>2</sub> signals displayed in top panel.

of the shape parameter. One particular type of distribution which can be modeled via Weibull is Log-normal distribution. Log-normal distribution is of significant interest because grain size distribution is naturally a Log-normal distribution.

The probability density function (PDF) for Weibull distribution is given as:

$$f(x;\lambda,k) = (k/\lambda)(x/\lambda)^{k-1}\exp[-(x/\lambda)^k]x \geq 0 \quad , \quad (1)$$

$k > 0$  shape factor,  $\lambda > 0$  scale factor.

Most of the NMR  $T_2$  distributions of our samples display bimodal behavior, so we add up two Weibull distributions with different weighting factors  $\alpha$  as:

$$E(x;\lambda_1,k_1,\lambda_2,k_2,\alpha_1,\alpha_2) = \alpha_1 f_1(x;\lambda_1,k_1) + \alpha_2 f_2(x;\lambda_2,k_2) \text{ where } \alpha_1 + \alpha_2 = 1 \quad . \quad (2)$$

The normalized error or objective function for the VFSA optimization is as follows:

$$E(x;\lambda_1,k_1,\lambda_2,k_2,\alpha_1,\alpha_2) = 2 \sum_{i=1}^n [f(x_i) - \text{NMR } T_2(i)] / \sum_{i=1}^n [f(x_i) + \text{NMR } T_2(i)] \quad . \quad (3)$$

NMR  $T_2$  data are discretized in the  $T_2$  domain with  $n$  as the number of total samples and  $x$  is:

$$x = \ln(T_2/T_{2,0}) \quad . \quad (4)$$

$T_{2,0}$  is the smallest  $T_2$  used in the  $T_2$  distribution (here 0.01 ms). There are five independent model parameters, i.e.,  $\lambda_1, k_1, \lambda_2, k_2, \alpha_1$ , to fit for each core plug. It worth noting that the extension of this approach to tri-modal distribution is straightforward where there will be 8 model parameters to fit the NMT  $T_2$  distribution. The fitting can be formulated as a constrained non-linear optimization which we addressed via VFSA in this paper. Fig. 3 shows the evolution of optimization algorithm to retrieve model parameters for one of the core plugs. As can be seen, in less than 160 iterations all of the model parameters are converged. We repeated the optimization process with different random initial guess for model parameters and confirmed that VFSA is able to find consistent model parameters. The optimized model parameters have been used in decomposing the NMR  $T_2$  response of all core plugs and then vuggy and microporosity of each core plug computed. Fig. 4 illustrates the NMR distribution and the associated bimodal Weibull distribution fits for one of the core plugs.

Analyzing the NMR response of all core plugs, we conclude that on average vugs contribute 80-95 percent of NMR total porosity and only a small fraction associated with microporosity. The NMR measurements provide convincing evidence that a dual pore system exists in these core plugs consisting of a connected microporosity with vugs. This information is vital for the SDEM resistivity and velocity modeling in the next part.

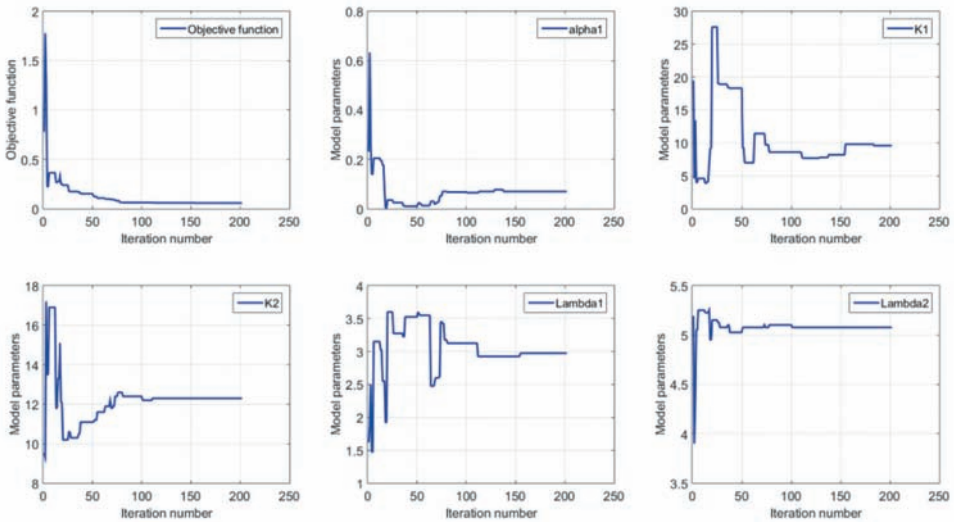


Fig. 3. The evolution of the error function and model parameters for NMR curve-fitting exercise using VFSA optimization.

## RESISTIVITY MODELING

Pore structure dominates the petrophysical properties of the carbonates. Pore combination modeling (PCM) is a general methodology to model the influence of pore geometry on resistivity and permeability. PCM is consistent with Archie's equation (Myers, 1989, 1991) but represents an extension allowing effect of multiple pore systems to be modeled. The empirically determined parameters in Archie's equation are correlated with pore geometry. Myers (1991) developed quantitative relation between thin section point counts and Archie's parameters for different pore systems (vuggy, intergranular, and microporosity) for a global carbonate data set. This model for nonconductive inclusions represents a special case of conductive inclusions. Using this technique the effects of individual pore system can be isolated. The following equation can be used for a dual pore system as the case of this paper. Extending the PCM modeling to three or more pore systems is straightforward.

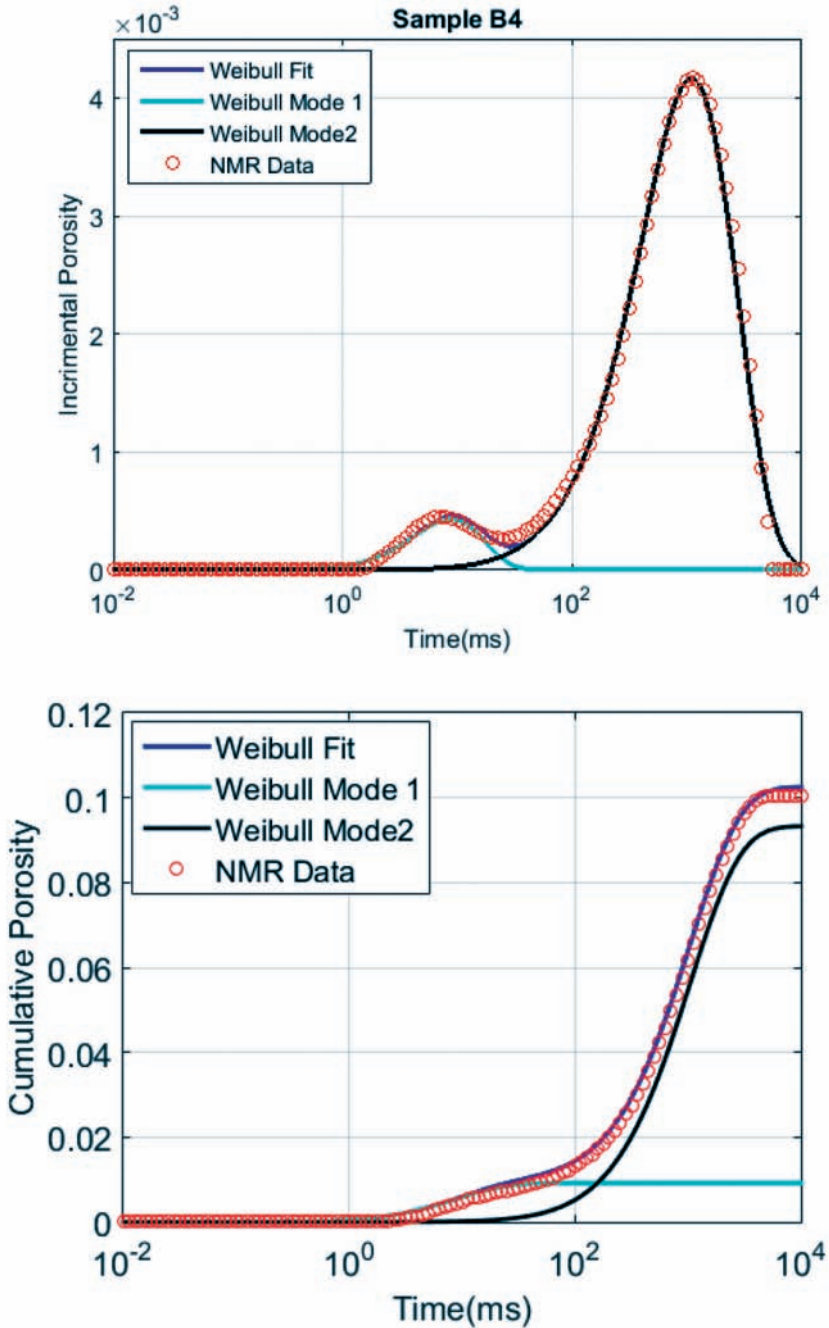


Fig. 4. Top panel shows NMR  $T_2$  distribution and the associated bimodal Weibull distribution fit. The dots are NMR measurements (10 porosity unit). The solid black line is Weibull fit to the second mode or pore type which are vugs (9 porosity unit). The cyan solid line is the Weibull distribution of the first mode or pore type which is microporosity (less than 1 porosity unit). The bottom panel shows the cumulative distribution of NMR  $T_2$  signal displayed in top panel.

$$F = (1/\phi_m)^{\lambda_m} (\phi_m/\phi_t)^{\lambda_v} \tag{5}$$

Here, F is the formation factor,  $\phi_m$  is the fraction of microporosity,  $\phi_t$  is the total porosity  $\phi_t = \phi_m + \phi_v$ , and  $\phi_v$  is the vuggy porosity.  $\lambda_m$  and  $\lambda_v$  are the lithology exponents for microporosity and vugs, respectively. The formation factor versus total Archimedes porosity is plotted in Fig. 5. The different blue lines all extrapolated to  $F = 1$  and  $\phi_t = 1$  are for  $\lambda_m$  from zero to three. One of these lines (red one) is the microporosity line best explained the petrophysical characteristics of these core plugs. There is a large scatter of these data about any of the lines because there are two pore types present and the amounts of both are changing. Fig. 6 displays the same data plotted in  $F-\phi$  log-log plane. The microporosity trend line selected for the data set is obtained from the non-linear optimization. The position that vuggy porosity lines intersect the microporosity line will provide the amount of each individual porosity. The vuggy porosity computed from resistivity modeling along with the vuggy porosity derived from velocity modeling will be used later in an inversion machine to optimize model parameters of both velocity and resistivity models.

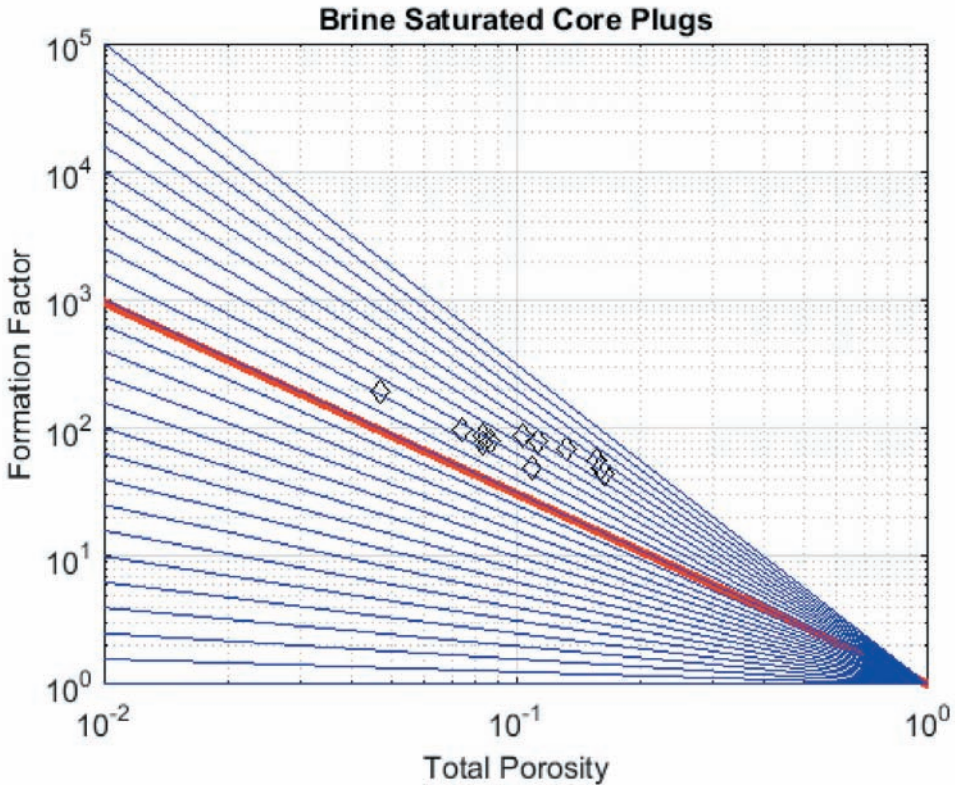


Fig. 5. Plot of the formation factor versus Archimedes porosity. No trend exists because there is a dual pore system of micro-pores and vugs.



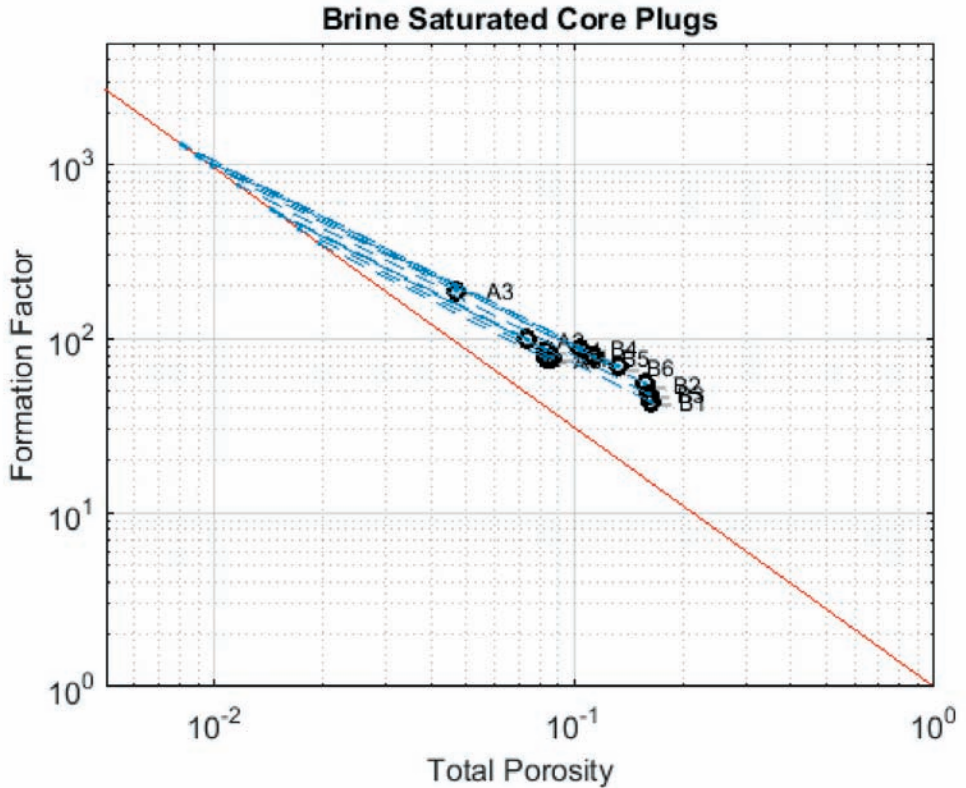


Fig. 6. Plot of the formation factor versus Archimedes porosity. The optimum microporosity lithology exponent (red line) is obtained from non-linear optimization. The dashed blue lines are optimum lithology exponent for vugs.

### VELOCITY MODELING

Historically the Reuss and Voight averages have been used to relate the modulus of the components of a rock to its resultant modulus of the mixture. They however only represent bounds on the moduli of the material mixtures. The actual modulus lies somewhere in between these bounds. To further refine these averaging techniques and by including additional textural information, Myers and Hathon (2012), developed a Staged Differential Effective Medium (SDEM) model for velocities. This starts by calculating the properties of a dilute mixture. Inclusions are added to a host while assuming they only feel the average properties of the host and neglecting interaction terms between the inclusions.

Critical concentration models (Nur et al., 1995) are naturally included in their models. The first integration step is from pure host to the critical concentration with an  $L = 0$  (iso-stress average). Then the integration is extended to the final porosity with a non-zero value of  $L$ :

$$M = M_c \{ 1 + [(\phi_c - \phi) / \phi_c] \cdot [(M_i - M_c) / M_c] \cdot L \} / \{ 1 - [(\phi_c - \phi) / \phi_c] \cdot [(M_i - M_c) / M_i] \cdot (1 - L) \} \quad (6)$$

This is a two-stage SDEM model for the rock;  $\phi_c$  is the critical porosity,  $M_i$  is the modulus of the inclusion,  $L$  the SDEM model parameter associated with this inclusion, and  $M_c$  is the iso-stress (Reuss) average of the host and grain modulus.

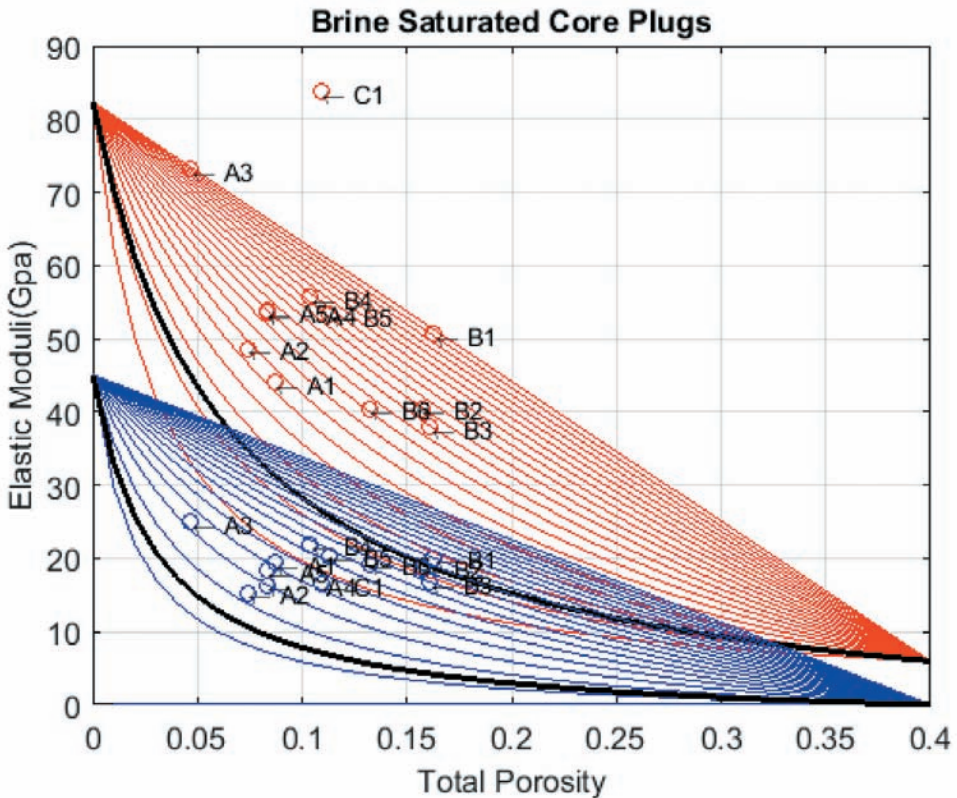


Fig. 7. Bulk and shear moduli versus Archimedes porosity. The red lines (bulk moduli) and blue lines (shear moduli) are for  $L = 0$  to  $L = 1$  spanning all the data unless C1 sample which is associated with an erroneous reading in P-wave traveltime. No trend exists because there is a dual pore system of micro-pores and vugs. The black curves are the optimum microporosity fits to the data.

In general, SDEM allow continuous interpolation between iso-strain and iso-stress averages of the moduli and provide a framework to include multiple lithology changes at separate integration steps. SDEM generates fluid substitution which are consistent with Gassmann's equation. The staged DEM models therefore represent an extension to Gassmann's equation which allows multiple minerals and pore geometries to be included.

Fig. 7 illustrates the Reuss and Voight average bounds for the carbonate core plugs. Different values of L for both bulk and shear moduli are also depicted. One of these lines (black) is the microporosity line that best explained the moduli of these core plugs. Like the resistivity model there is no obvious trend in these data because there are two pore types present and the amounts of both are changing. Fig. 9 displays the same data as shown in Fig. 7. The microporosity and vuggy porosity trends selected for the data set are obtained from the non-linear optimization of velocity and resistivity data. The position that vuggy porosity lines intersect the microporosity line provides the amount of each individual porosity. The vuggy porosity computed from velocity modeling along with the vuggy porosity derived from resistivity modeling will be used later in an inversion machine to optimize the model parameters of both velocity and resistivity models.

### NON-LINEAR INVERSION TO OPTIMIZE SDEM MODEL PARAMETERS

To optimize the SDEM model parameters, we define an objective function as the difference between vuggy porosities predicted from resistivity modeling ( $\phi_i^{vr}$ ) and the vuggy porosities computed from velocity modeling ( $\phi_i^{vk}, \phi_i^{vs}$  for bulk and shear moduli, respectively) to be minimized. Index i indicates core plug numbers from 1 to n. During the optimizations process several constrained are applied. For instance, the computed moduli have to be always between Reuss and Voight average bounds. Microporosity curve in velocity modelling has to intersect vuggy porosity line for all the core plugs. Microporosity line in resistivity modeling has to intersect vuggy porosity line for all the core plugs.

$$E(\phi^c, M_k, M_s, \lambda_m, \lambda_v, L_{ms}, L_{mk}) = 2 \sum_{i=1}^n [\phi_i^{vk} - \phi_i^{vs}] / \sum_{i=1}^n [\phi_i^{vk} + \phi_i^{vs}] + 2 \sum_{i=1}^n [\phi_i^{vk} - \phi_i^{vr}] / \sum_{i=1}^n [\phi_i^{vk} + \phi_i^{vr}] \quad (7)$$

SDEM model parameters are critical porosity ( $\phi^c$ ), bulk ( $M_k$ ) and shear ( $M_s$ ) moduli of grains, microporosity lithology exponent for resistivity ( $\lambda_m$ ), vuggy porosity lithology exponent for resistivity ( $\lambda_v$ ), microporosity parameter

for shear modulus ( $L_{ms}$ ), microporosity parameter for bulk modulus ( $L_{mk}$ ). Vuggy porosity L parameters for bulk and shear moduli are set to 1.0 based on the previously published results (Myers and Hathon, 2012). Table 1 summarizes all the model parameters as well as their mean values for 200 runs of VFSA each with 200 iterations. Fig. 8 shows the optimization path to predict the microporosity lithology exponent associated with resistivity and the microporosity L parameter associated with bulk modulus. Fig. 9 illustrates petro-elastic rock physics template. Fig. 10 displays the correlation of vuggy porosity estimated from velocity and resistivity. It also shows a high correlation between vuggy porosity jointly estimated from velocity-resistivity and the ones estimated from NMR and  $\mu$ CT measurements.

Table 1. SDEM model parameters. Note that vuggy porosity L parameters for bulk and shear moduli are set to 1.0 based on the previously published results (Myers and Hathon, 2012). The rest of parameters are obtained from VFSA optimization.

SDEM Model Parameters	Mean Value
Critical porosity	0.40
Bulk Modulus (Gpa)	82.35
Shear Modulus (Gpa)	45.08
L parameter for microporosity associated with bulk modulus	0.07
L parameter for microporosity associated with shear modulus	0.07
L parameter for vuggy porosity of bulk modulus	1.00
L parameter for vuggy porosity of shear modulus	1.00
Lithology exponent for microporosity associated with resistivity	1.49
Lithology exponent for vuggy porosity associated with resistivity	1.06

## CONCLUSIONS

An integrated technique is proposed to jointly model the resistivity and velocities measurements using SDEM for dual porosity carbonates. One of the salient features of this approach is its consistency in predicting vuggy and matrix porosities from different data sources. The other significant feature of the proposed method is the calibration of petro-elastic and petro-electric models against NMR and  $\mu$ CT measurements. The technique has been successfully applied on carbonate core plugs from northern Niagaran reef. The major pore system in these samples are vugs. Microporosity only contributes about 1 to 2 porosity unit. Optimization algorithm has been able to fine tuned the model parameters of resistivity and velocity and provides vuggy and matrix porosities close to NMR and  $\mu$ CT estimated porosities.

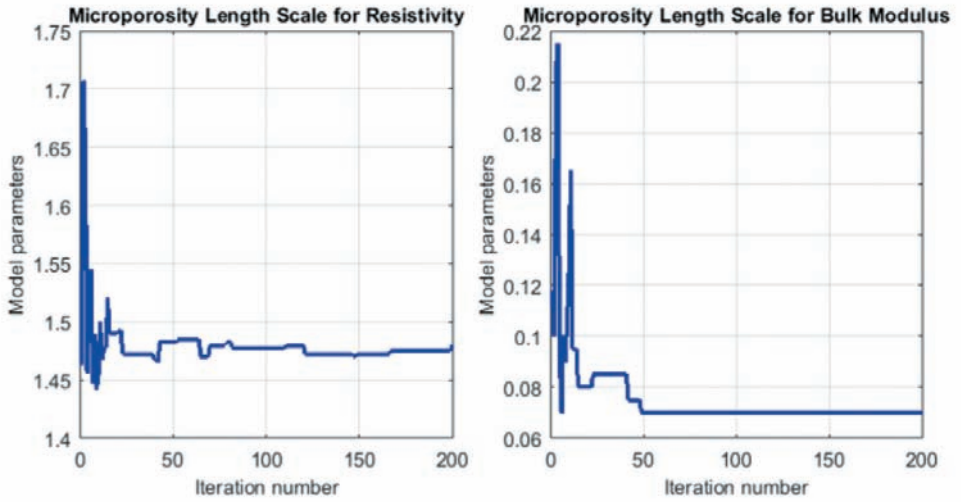


Fig. 8. VFS optimization of two model parameters. The left panel is the microporosity lithology exponent associated with resistivity. The right panel is the microporosity L parameter associated with bulk modulus.

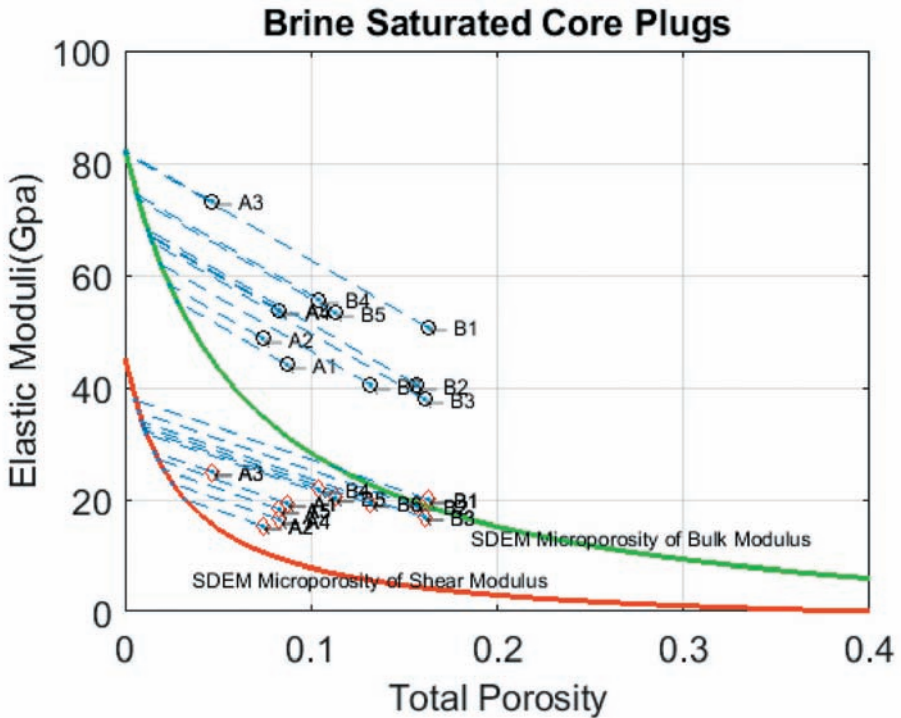


Fig. 9. Bulk and shear moduli versus Archimedes porosity. The optimum microporosity L parameters (red for shear and green for bulk modulus) are obtained from non-linear optimization. The dashed blue lines are drawn using the  $L = 1$  for vugs.

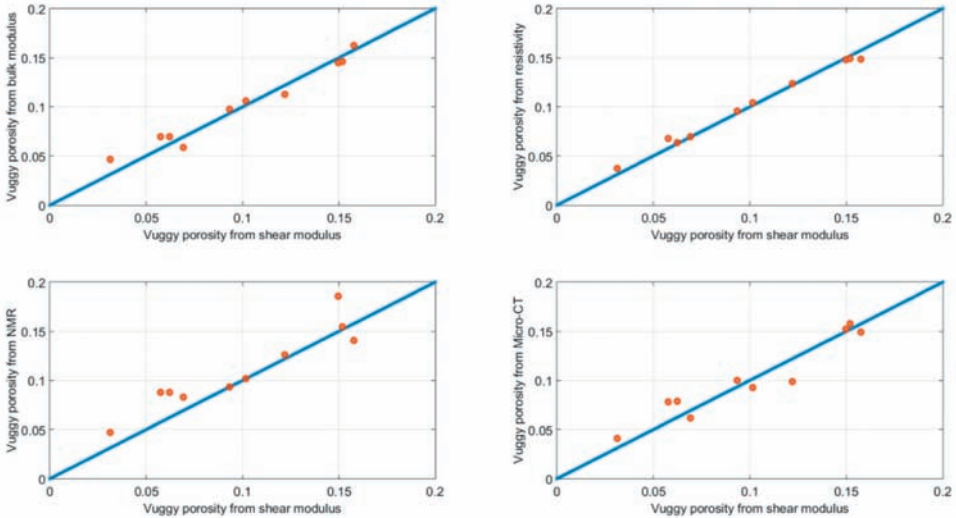


Fig. 10. Comparison of vuggy porosities estimated from different methods. The bottom panels indicate high correlations between velocity-derived vuggy porosity (shear modulus here) and vuggy porosity forms independent measurements of NMR and micro-CT.

Our future work is to extend this methodology to well logs and seismic data. The calibrated rock physics templates using well logs and core plug measurements ( $\mu$ CT, NMR, Resistivity, Ultrasonic) will be generated and will be used to convert pre-stack seismic inversion products to pore type and pore volume.

## ACKNOWLEDGEMENT

We would like to thank the Capstone team at the University of Houston for making some of the measurements on the core plugs.

## APPENDIX

### VERY FAST SIMULATED ANNEALING (VFSA) OPTIMIZATION

In order to avoid the problem of local minima in the inversion process, a global optimization method is preferred. We intend to use Very Fast Simulated Annealing (VFSA), one of the variants of Simulated Annealing (Ingber, 1989, 1993). VFSA draws a new sample in model space from a temperature-dependent 1D Cauchy distribution via a Monte Carlo guided search. The advantage of this method is that it has a higher chance to find the global optimum of the objective function. SA is an approach which is analogous to a physical process in which a solid in a "heat bath" is heated by increasing the temperature, followed by slow cooling until it reaches the global minimum energy state.

The original Metropolis algorithm is analogous to taking a random walk in the model space. At each step the change in the "energy" ( $\Delta E$  = error function in optimization process) is calculated for the entire system. The model is accepted if  $\Delta E < 0$ . If  $\Delta E > 0$ , then the new model is accepted with a weighting function  $\exp(-\Delta E/T)$ , where T is the temperature. Finally, the temperature is slowly lowered during the execution of the algorithm. Random perturbations according to these rules eventually cause the system to reach equilibrium. Several geophysical applications of SA and VFSA can be found in Sen and Stoffa (1995).

## REFERENCES

- Myers, M. T., 1989. Pore combination modeling: Extending the Hanai-Bruggeman equation. Abstr., SPWLA 30th Ann. Logg. Symp., Denver.
- Nur, A., Mavko, G., Dvorkin, J. and Gal, D., 1995. Critical Porosity: The Key to Relating Physical Properties to Porosity in Rocks. Expanded Abstr., 65th Ann. Internat. SEG Mtg., Houston: 878.
- Myers, M.T., 1991. Pore combination modeling: A technique for modeling the permeability and resistivity of complex pore systems. Abstr., SPE Mtg., Dallas: 22662.
- Myers, M.T. and Hathon, L.A., 2012. Staged differential effective medium (SDEM) models for the acoustic velocity in carbonates. *Transact. ARMA*, 12: 553.
- Archie, G.E., 1962. The electrical resistivity log as an aid in determining some reservoir characteristics. *Transact. AIME*, 146: 54-67.
- Ingber, L., 1989. Very fast simulated re-annealing. *Mathemat. Comput. Modell.*, 12(8): 967-973.
- Ingber, L., 1993. Simulated annealing: Practice versus theory. *Mathemat. Comput. Modell.*, 18(11): 29-57.
- Sen, M.K. and Stoffa, P.L., 1995. *Global Optimization Methods in Geophysical Inversion*. Elsevier Science Publishers, Amsterdam.